

Analysis of Fault Injection in Implantable Capacitive Blood-pressure Sensors

J. A. Miguel, Y. Lechuga and M. Martinez

*Technology Electronics, Automatic and System Engineering Department, University of Cantabria,
Avda de los Castros s/n, Santander, Spain*

Keywords: MEMS Testing, Fault Injection, Fault Modelling, Finite-element Analysis, Capacitive Pressure Sensor.

Abstract: This work explores the fault injection problem in the particular case of an implantable capacitive micro-electromechanical pressure sensor for blood-flow measurement applied to the detection of in-stent restenosis. In order to develop a MEMS testing method for this sensor and its related electronic circuitry, an accurate and realistic fault model is essential. A behavioural description of the equivalent capacitance in the fault-free case can be obtained from the analytical and numerical solutions of the deflection of a circular diaphragm under a uniformly distributed pressure. However, the deflection problem for faulty conditions due to, for example, contamination-based defects or partially released structures must be solved and modelled using finite-element analysis.

1 INTRODUCTION

Vascular diseases are the leading mortality cause in the European Union, being responsible of the 40% of all deaths in the year 2008 (OECD, 2010). The use of angioplasties and vascular stents has become the most frequently used method for the treatment of the most common vascular illness, such as blood vessels stenosis, aortic aneurysms, arteriosclerosis and renovascular hypertension.

However, in-stent restenosis (ISR), due to neointimal tissue growth inside an implanted stent, keeps on being the major drawback in stent implantation, seriously compromising its long-term results. The recent appearance of the so called intelligent stents involves a potential economical solution to this problem. An intelligent stent (e-stent) incorporates a sensor capable of monitoring and transmitting real-time measurements of biological parameters related to blood-flow quality. There are three typical approaches for designing the aforementioned intelligent stents, regarding the nature of the biological parameters and the way they are measured: capacitive pressure measurements, electromagnetic blood flow measurements and ultrasonic blood flow measurements.

It is important to point out that an implantable sensor for any of these techniques must match

certain characteristics, including reduced size, output stability, low power consumption, low cost and above all, reliability over extended time period. This fact makes testing and thus, realistic fault injection and fault modeling, a critical issue.

The objective of this work focuses on fault model generation for an implantable capacitive MEMS pressure sensor utilized to measure blood-flow velocity. This model will allow the future development of a comprehensive MEMS testing methodology.

Continued success for MEMS will require cost-effective methods of manufacturing. Advances in this area must include a testing methodology that allows products to be economically tested while ensuring high quality and reliability. This is especially important in applications where MEMS are integral parts of safety-critical systems such as implantable biomedical devices.

Traditionally, manufacturers focus on partially checking the functionality of MEMS by performing certain electrical, optical, mechanical or environmental measurements (Wang et al., 2008). However, there is a need to obtain correlations between failure modes and the underlying physical causes. These relationships will allow accurate modeling of complex effects that can be used in fault model generation, fault diagnosis and in the development of efficient testing techniques.

Thus, success of any MEMS testing methodology is highly dependent on the fault models employed. Fault models that do not include real defective behavior can reduce defect coverage, degrade test quality and, therefore, the reliability of the implantable sensor.

MEMS fault models must explicitly consider the impact of defects on the micromechanical structures. Our approach centers on the inductive generation of the possible faulty behaviors from realistic finite-element simulations. Particularly for those faults whose behavior cannot be easily described by an analytical model, as in the fault-free case.

Section 2 introduces the most common failure mechanisms that can affect MEMS devices. In Section 3 the capacitive pressure sensor chosen as system under test is presented. Section 4 describes the need of finite-element (FE) analysis for modeling faults such as incomplete release of suspended elements and contamination, in the case of diaphragm or membrane-based MEMS pressure sensors. Finally, in Section 5 conclusions are presented.

2 FAILURE MECHANISMS AND FAULT CLASSES

Among the failure mechanisms or defects which can appear during fabrication, defects occurring during the CMOS process can be distinguished from defects occurring during micromachining (Castillejo et al., 1998); (Mir et al., 2000); (Huang et al., 2012).

Microelectronic and micromechanical components are created on the wafer during the CMOS process by means of a set of semiconductor, conductor and dielectric layers. These layers are obtained through technological operations such as: oxidation, deposition, photolithography, etching, ion implantation or annealing. Each one of them is a potential source of defects. Therefore, as a result of a technological step, contaminants or residuals may remain in the environment and be harmful in a succeeding step.

For example, one of the most common problems encountered for the fabrication of CMOS-compatible MEMS is the presence of oxide residuals in areas of naked silicon exposed for micromachining. These oxide residuals can be formed from thermal silica and from different layers of oxides which have not been properly cleaned, and can prevent the formation of an adequate cavity during micromachining of the exposed silicon.

During micromachining, anisotropic etching outside the foundry is used to suspend the structures. For surface micromachining, a sacrificial layer of a material such as silicon oxide, polysilicon, porous silicon or aluminium is deposited. The postprocessing operation removes this sacrificial layer to suspend the microstructure. However, a suspended microstructure may not be fully released, or the cavity produced may be inadequate, due to several mechanisms that include, not only the presence of unwanted oxide residuals, but also insufficient etching time, slow etching rate because of an inadequate solution, re-depositions after etching, or the formation of complex substances from etching chemical reactions. These substances may affect the quality of the solution, reducing etching rate or appear stuck on the microstructure at the end of the process.

Failure mechanisms can be classified according to the physical properties or parameters of the MEMS which are affected. In summary, each group of faults (affecting the gauge that provides the actual electrical interface or the microstructure that suspends the gauge) is in turn classified in two classes: catastrophic faults, which prevent any system utilization, and parametric faults, for which changes on geometrical or material parameters alter microsystem performance.

Stiction to the bulk or the inadequate release due to incomplete etching of a suspended structure can mostly occur for both surface and bulk micromachining. With such faults, a seismic mass may remain stuck, for example, in the case of an accelerometer, or the geometry and clamping conditions of the membrane of a capacitive pressure sensor may be significantly affected. Besides that, particle contamination may also give rise to catastrophic or parametric faults, depending on their position, geometry, and size.

For example, highly anisotropic wet etching of single crystal silicon is widely used to create membranes. Impurities or small crystal lattice defects in the bulk material encountered during this process have been reported to cause pyramids on top of the membrane that change its characteristics (Landsberger et al., 1996). The maximum size of the pyramids is dependent on the depth of the etch into the bulk and at which depth the defect occurs. The angles between the main crystal planes of single crystal silicon determine the sidewall slope of a pyramid. FE-based fault characterization is particularly important for these defects whose real effect over MEMS performance cannot be easily derived from analytical expressions.

3 CAPACITIVE PRESSURE SENSOR

Blood flow measurement represents one of the most common procedures performed in hospitals for the monitorization of cardiovascular diseases. In this sense, an intelligent stent that incorporates a sensor capable of monitoring and transmitting real-time measurements of biological related parameters for its clinical consultation can help to detect in-stent restenosis (ISR).

Among the three typical flow measurement approaches compatible with intelligent stent design (electromagnetic, ultrasonic and pressure-based) we focus on the pressure-based measurement since it provides not only a measurement of the blood-flow velocity into an obstructed vessel, but also a measurement of the absolute pressure in the vessel, providing additional information to carry out ISR monitorization.

The simplest implantable version of the pressure sensor is made of a capacitive MEMS to measure blood pressure, and an inductance to form the LC tank that transmits the information by proximity coupling (Takahata et al., 2006). This capacitive MEMS approach allows the integration of the sensor and the electronic circuits in the same silicon substrate, decreasing the overall cost of the system. The low energy requirements of its components help to reduce the system size since it can be powered by a wireless link.

The principle of operation of this kind of sensors is based on the simple concept of a two parallel plate capacitor, where the equivalent capacitance is inversely proportional to the distance between the plates. Actually, these sensors usually consist of a fully clamped diaphragm membrane suspended over a sealed cavity and a fixed backplate. Once some pressure is applied to the flexible membrane, it suffers a deformation that reduces the chamber size, increasing the equivalent capacitance between the two-plate structure.

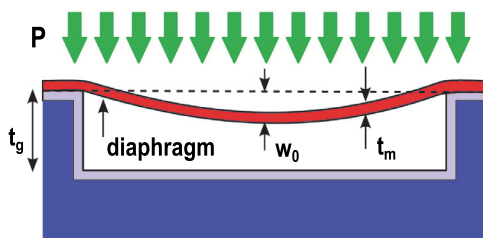


Figure 1: Simplified cross-section of the capacitive sensor.

Fig. 1 shows a simplified cross-section of a MEMS capacitive pressure sensor, based on a deflecting diaphragm and a fixed backplate; where P is the uniformly distributed pressure applied to the diaphragm, w_0 is the deflection of the diaphragm center, t_g is the initial undeflected gap between the plates and t_m is the thickness of the diaphragm.

Once known the analytical expression of deflection (in radial or geometric coordinates) of a fully clamped circular or rectangular diaphragm, the capacitance of the sensor can be analytically calculated by:

$$\Delta C = C_S - C_0 = \iint_A \frac{\epsilon_0 dx dy}{t_g - w(x, y)} - \epsilon_0 \frac{A}{t_g} \quad (1)$$

Where C_0 is the capacitance of the undeformed sensor, ϵ_0 is the dielectric permittivity of free space and A is the area of the plates.

In this work we are going to focus on the case of a circular diaphragm model in order to evaluate the necessity of a finite-element analysis for accurate fault injection and simulation.

3.1 Circular Diaphragm

The deflection of a circular diaphragm with fully clamped edges can be analytically expressed as a function of the radial distance from the center of the plate (Timoshenko, 1940). To validate the analytical model, the following assumptions must be considered (Chang et al., 2002): (a) the material of the diaphragm must have isotropic mechanical properties; (b) the thickness of the metallic electrode on the plate has to be smaller than the plate's thickness in order to be neglected; (c) the gap between the flexible plate and the backplate needs to be small compared with the lateral extents of the plates, so that the electric field fringing effects can be neglected; (d) the residual stresses in the flexible plate are not taken into consideration. Once the previous requirements have been fulfilled, the relationship between the circular diaphragm's deflection and the radial distance can be stated as:

$$w(r) = w_0 \left[1 - \left(\frac{r}{a} \right)^2 \right]^2 \quad (2)$$

Where r is the distance from the center of the diaphragm, a is the radius of the diaphragm and w_0 is the maximum center deflection.

The value of the maximum center deflection presents different analytical approximations, regarding the relationship between the deflection

and the thickness of the diaphragm. Under small deflection conditions ($w_0 < 30\% t_m$), the maximum deflection of a circular thin plate with fully clamped edges can be noted as:

$$w_0 = \frac{3Pa^4(1-\nu^2)}{16Et_m^3} \quad (3)$$

Where a is the radius of the diaphragm, P is the applied pressure, and ν and E are the Poisson ratio and the elasticity modulus of the diaphragm's material respectively.

Under large deflection conditions ($w_0 > 30\% t_m$), the relationship between the maximum center deflection of the plate and the uniformly applied pressure can be denoted as a cubic equation:

$$w_0 = \frac{3Pa^4(1-\nu^2)}{16Et_m^3} \cdot \frac{1}{1 + \frac{0.488w_0^2}{t_m^2}} \quad (4)$$

It can be seen how equation (4) can be approximated to (3) when $w_0 \ll t_m$. For this reason, equation (4) can be used to simulate the behaviour of the sensor in both small and large deflection circumstances.

4 FE FAULT INJECTION

Finite element analysis (FEA) techniques are essential for the design of micromechanical structures. FEA tools work at a low level, are processor intensive and incompatible with electronic circuit simulators. This means that the designer lacks the modelling tools to design without extensive experimentation. In this sense, other approaches are required to enable closed-loop simulation of the complete microsystem containing sensors or actuators together with electronic feedback, processing and biasing circuits. For this reason, designers and test engineers are increasingly concerned about the introduction of behavioural languages developed for circuit modelling and compatible with electric simulators.

The use of through and across variables enables the simulation of forces and displacements (or other physical quantities) in a similar way to currents and voltages. Closed-loop, network type, simulations of transducers and electrical circuitry within the same simulation environment is therefore possible (Teegarden et al., 1998); (Mukherjee et al., 1999).

For accurate fault simulation results, it is essential for the faults model to be correct. We

propose the use of a finite-element CAD tool to analyze the effect of defects that can occur during the manufacturing process, or even during the useful lifetime of a capacitive MEMS pressure sensor, to establish which ones will give rise to a faulty behaviour, and to accurately describe them, and the whole system, by a electrical-compatible behavioural model where future test methods can be evaluated.

To enable fault simulation with a realistic estimation of the fault coverage of a test method, a complete library of fault models, based on actual defects/failure mechanisms, has to be developed.

Because of its relatively small thickness and high deflection, the diaphragm or membrane of the capacitive pressure sensor is expected to be the most vulnerable component regarding the appearance of defects. It has therefore been chosen as the critical element of the capacitive sensor. The sensor simulated consists of a polysilicon diaphragm (Young Modulus: $E = 169$ GPa; Poisson Coefficient: $\nu = 0.22$) with a thickness of $4\mu\text{m}$, a radius of $350\mu\text{m}$ and a sealed cavity of $2\mu\text{m}$ height.

A uniformly distributed pressure of 60 mmHg is applied to the top of the membrane. This pulmonary artery pressure value is related to a medical condition of moderate stenosis.

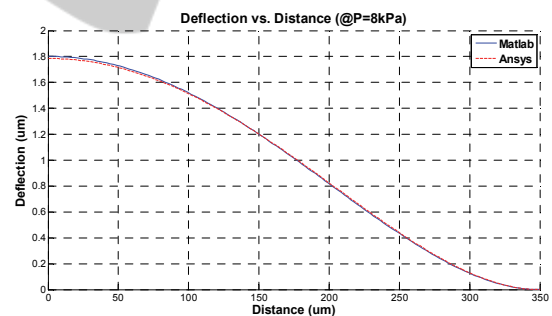


Figure 2: Behavioural model vs finite element model.

A behavioural model for the membrane deformation in the fault-free case has been developed using the equations (2) and (4) under a Matlab simulation environment. Fig. 2 shows the deflection results regarding the distance from the center of the membrane obtained with this behavioural model compared to the ones from a FE simulation. When building a FE model of the membrane, we must consider it as a circular-shaped thin plate, which is clamped on all edges in such a way that no movement or rotation is allowed in all directions (restricted in all degrees of freedom).

Fig. 2 shows that the error caused when using the analytical approximation instead of the finite-

element model becomes slightly higher as far as we come closer to the center of the membrane. The maximum deflection calculated through the Matlab model has a value of 1.802 μm , whereas this result reaches 1.785 μm for the FE model. However, the accuracy of this approximation can be enhanced, if needed, without mayor changes in its mathematical formulation. Therefore, an analytical-based model can be considered valid for modelling the fault-free behaviour of the membrane.

Finite element simulation is also carried out on a representation of the membrane with a defect inserted. For different sizes and locations of defects this is repeated and the deflection produced is measured. Because of the symmetry of the membrane, fault injection is only necessary all along one radius of the membrane, simplifying fault injection and reducing simulation time.

As said in Section 2 impurities or small crystal lattice defects cause pyramids on top of the membrane. The angles between the main crystal planes of single crystal silicon determine the sidewall slope of a pyramid (54.7°, the angle between a {100} and a {111} plane in case of anisotropic etching of a {100} oriented wafer). This is therefore a fixed parameter. Altering the base length of the pyramid, the size is also changed, since the height of the pyramid is calculated from the fixed sidewall slope (Landsberger et al., 1996); (Rosing et al., 2002).

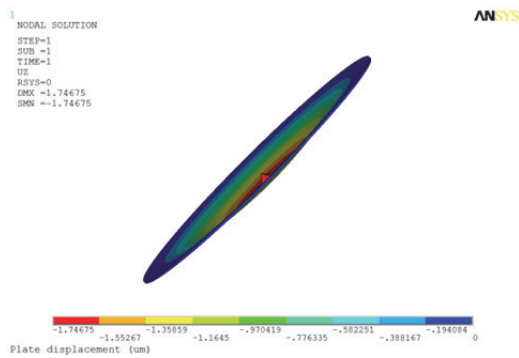


Figure 3: Screenshot of membrane with pyramid.

Pyramids on the membrane have been modelled to have: a) the same size but locations all along a radius of the membrane; and b) different sizes on the same position in the centre of the membrane. An example of a membrane with a pyramid, deflected under the applied pressure, is given in Fig. 3. The different colours are different regions of deflection of the membrane.

Fig 4 shows the simulations of the displacement of the center point of the membrane (maximum

deflection) in relation to different locations of a pyramid (base side: 30 μm) over the radius line of the membrane. We can highlight the significant drop in displacement when the pyramid is located close to the center of the membrane. Therefore the strongest impact of a pyramid is produced at that location. If a pyramid is located closer to the edge of the membrane, the influence on the deflection gets smaller. However second order effects related to the proximity to the clamped edge and variations in the effective geometry of the membrane (areas of maximum stress) make the maximum deflection to decrease, contrary to what could be expected, for pyramids approaching the edge of the membrane.

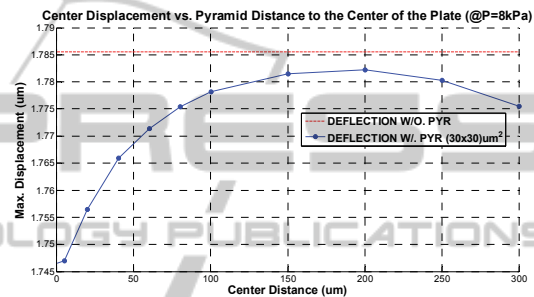


Figure 4: Center deflection vs pyramid location.

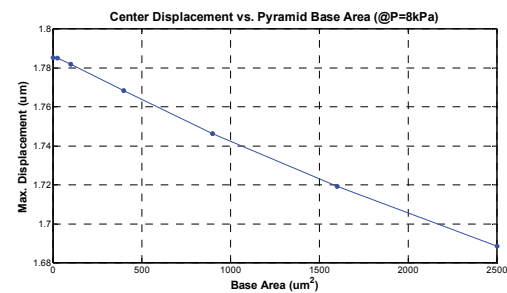
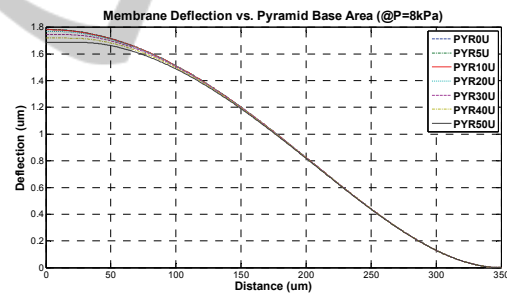


Figure 5: Deflection for pyramids located at the center.

The next step is to place the pyramid in the center of the membrane while only its size is varied. The base length of the pyramids has been varied in the range from 5 to 50 μm . The simulation results are shown in Fig. 5. As can be seen in the lower graph, the displacement of the centre point of the

membrane approximates a linear function, as it steadily decreases with increasing pyramid size. The upper graph in Fig. 5 shows the membrane deflection for different pyramid sizes. One important aspect to point out is the constant maximum deflection value for the membrane, not at a single point, but under the complete pyramid base area. This last effect cannot be modelled by using the mathematical formulation presented in Section 3, even if we modify it to increase its accuracy in order to get closer to the results obtained by FE analysis.

Fig. 4 and Fig. 5 also show that the presence of a pyramid on top of the membrane of our capacitive MEMS pressure sensor produces a smaller deflection than expected in the fault-free case. Thus, this faulty condition implies a sensitivity loss of the sensor that can compromise its reliability, which is a critical issue for implantable devices.

Therefore, it is important to count on an accurate behavioural model for its main component, the membrane, valid for both fault-free and faulty conditions. As said before, its deflection can have an acceptable analytical solution in the fault-free case. However, in this work we have proven that this mathematical formulation is no longer valid for modelling the membrane with certain kinds of faults as, for example, the formation of pyramids on top of the membrane. Therefore it is necessary to create additional mathematical models that accurately describe the behaviour of the membrane under faulty conditions, considering the deflection results obtained through FE simulations. Especially for those faulty cases which significantly affect the geometry and/or material properties of the membrane.

5 CONCLUSIONS

In this work test-related problems for implantable capacitive MEMS pressure sensors for the early detection of in-stent restenosis have been presented.

The typical failure mechanisms and defects that can give raise to the faulty behaviour of a microelectromechanical system have also been explained.

The deflection problem of circular membranes has been proven to be analytically or numerically solvable for a fault-free case, in order to build a behavioural model of the sensor. Nevertheless, this mathematical model is not valid to describe certain faulty conditions where the geometry or the material properties of the membrane are seriously affected. So as to obtain a realistic fault model in these cases a

finite-element analysis must be performed.

REFERENCES

- Castillejo A., Veychard D., Mir S., Karam J., Courtois B., Failure Mechanisms and Fault Classes for CMOS-Compatible Microelectromechanical Systems, *IEEE International Test Conference*, pp. 541–550, 1998.
- Chang S.-P., Lee J.-B., Allen M.G., Robust capacitive pressure sensor array, *Sensors and Actuators A: Physical*, vol. 101, pp. 231–238, September 2002.
- Huang Y., Vasani A. S. S., Doraiswami R., Osterman M., Pecht M., MEMS Reliability Review, *IEEE Transactions on Device and Materials Reliability*, vol. 12, no. 2, pp. 482–493, June 2012.
- Landsberger L. M., Nashed S., Kahrizi M., Paranjape M., On Hillocks Generated During Anisotropic Etching of Si in TMAH, *Journal of Microelectromechanical Systems*, vol. 5, no. 2, pp. 106–116, 1996.
- Mir S., Charlot B., Courtois B., Extending Fault-Based Testing to Microelectromechanical Systems, *Journal of Electronic Testing: Theory and Applications*, vol. 16, pp. 279–288, 2000.
- Mukherjee T., Fedder G. K., Blanton R. D., Hierarchical design and test of integrated microsystems, *IEEE Design and Test of Computers*, vol. 16 (4), pp. 18–27, 1999.
- OECD (2010), *Health at a Glance: Europe 2010*, OECD Publishing. http://dx.doi.org/10.1787/health_glance-2010-en
- Rosing R., Reichenbach R., Richardson A., Generation of component level fault models for MEMS, *Microelectronics Journal*, vol. 33, pp. 861–868, 2002.
- Takahata K., Gianchandani Y. B., Wise K. D., Micromachined antenna stents and cuffs for monitoring intraluminal pressure and flow, *Journal of Microelectromechanical Systems*, vol 15(5), pp. 1289–1298, October 2006.
- Teegarden D., Lorenz G., Neul R., How to model and simulate microgyroscope systems, *IEEE Spectrum* 35 (7), pp. 66–75, 1998.
- Timoshenko S., *Theory of Plates and Shells*, McGraw-Hill, New York, 1940.
- Wang L-T., Stroud C. E., Toubia N. A., *System-on Chip Test Architectures. Nanometer Design for Testability*, 1st. ed., Elsevier: Morgan Kaufmann Series, 2008.